Drilling of a Bidirectional Jute Fibre and Cork-Reinforced Polymer Biosandwich Structure: ANN and RSM approaches for Modelling and Optimization

Zohir Tabet
Universite du 20 aout 1955 de Skikda
Ahmed Belaadi (ahmedbelaadi1@yahoo.fr)
Universite du 20 aout 1955 de Skikda
Messaouda Boumaaza
Université 8 Mai 1945 Guelma
Mostefa Bourchak
King Abdulaziz University

Research Article

Keywords: Industrial fabrics/textiles, Sandwich structures, Delamination, Drilling/machining, RSM/ANN, Genetic algorithm optimisation

Posted Date: May 12th, 2021

DOI: https://doi.org/10.21203/rs.3.rs-503708/v1

Abstract

The present study examined the effects of drilling parameters such as spindle speed (*N*), feed rate (*f*), diameter of the tools (*d*) and drill geometry such as twist drills (HSS-TiN) and brad & spur drills (BSD) used on delamination damage in a biosandwich structure consisting of an epoxy matrix reinforced with bidirectional jute fibres and cork (JFCE). Response surface methodology (RSM) and artificial neural networks (ANNs) were exploited to evaluate the influence and interaction of the cutting parameters on the delamination factor (F_d) at the output during drilling. In addition, several optimization methods, such as desirability-based RSM, the genetic algorithm (GA) and the fmincon function, were applied to validate the optimal combination of cutting parameters (*f, N* and *d*) in the structures studied in biosandwiches during this research. According to the experimental results, severe damage was indeed observed with the BSD tool (F_d = 1.684) compared to the HSS-TiN tool (F_d = 1.555) for the same cutting conditions. To obtain the minimum F_d, the optimum conditions obtained by GA were respectively 1397.54 rev/min, 51.162 mm/min and 5.981 mm for HSS-TiN for *f*, *N* and *d*.

1. Introduction

Over the past twenty years, plant fibres have proven to be an attractive environmentally friendly alternative to glass fibres in organic matrix composites due to the growth potential of plant fibres in the industrial sector [1–3]. The use of natural fibres as a reinforcement for polymer matrix composites has aroused, in recent years, the interest of researchers and industrialists from an economic and ecological point of view [4, 5]. This use is justified, first, by the use of local resources, development of materials and taking into account the environmental impact technologies and the reduction of production costs while maintaining good performance compared to that of synthetic fibre (glass and carbon). On the other hand, this is due to the potential of natural fibres in terms of mechanical properties that can compete for certain types of plant fibres, with synthetic fibres commonly used in industry [6–8]. Natural fibres are initially biodegradable and are often considered neutral to CO_2 emissions into the atmosphere because their biodegradation produces only a quantity of carbon dioxide. Biocomposites are therefore easier to recycle. These are mainly used in many fields, such as construction, sports, and transport. Indeed, in order to better understand the behaviour of these biocomposites, in-depth scientific studies have been carried out by several researchers [9, 10]. Currently, there are a wide variety of plant fibres that are currently used as reinforcements for different matrices [11], such as sisal [12], jute [12, 13], *Agave americana L.* [14], flax [15, 16], *Washingtonia filifera* [17], *Luffa Vine* [18] and bamboo [19].

However, machining is also an important operation when preparing composite surfaces for bonding assembly for multi-material applications [20]. The machinability of composites mainly depends on the structure and intrinsic characteristics of the fibres and the mechanical properties between the fibres and the resin responsible for the creation of various defects during machining, especially delamination, cracking, uncut fibres and the tearing of fibres, which lead to rough surfaces [21–23]. In the case of biocomposites with biofibre reinforcement, the mechanical behaviour of the fibres must be taken into account since this behaviour is much more prominent than that of the matrix and because of the influence this behaviour will have on the final state of the machined part. Several research works have addressed machining during the drilling of composites with synthetic fibres of glass, aramid and carbon to study the mechanisms of interaction between the cutting tools and the material and identify the most influential machining parameters in relation to the behaviour of the fibres and thus choose the most suitable process [24–31]. However, the literature contains only a limited number of works dealing with machining biocomposites [22, 32, 41–50, 33, 51–56, 34–40] and comparative studies between biocomposites and composites

with glass fibres [57]. The phenomenon most studied by researchers is delamination during drilling. Indeed, several theories and techniques exist in the literature to determine the delamination factor [31, 32, 58, 59]. Indeed, standard high-speed steel twist drills (HSS) [37, 41, 42, 48, 54, 55, 60] or tungsten carbide (WC) [55] are the most common tools used. The drill point angle is usually chosen to be 118° with tool diameters ranging from 3 to 14 mm. There are also other types of tools tested for drilling biocomposites, such as a tungsten carbide brad drill [57] and an HSS drill with two cutting edges [42].

Aravindh and Umanath **[61]** used Taguchi's method in the case of drilling NFC biocomposites (jute, sisal and bamboo fibres) to determine the optimal drilling conditions to minimize delamination. The authors estimated the contributions of different elements under optimal drilling conditions, including drill diameter (88.19%), feed rate (7.64%) and spindle speed (2.62%). Drilling tests conducted by Mercy et al. [61] on epoxy reinforced with pineapple fibre biocomposites at different orientations were performed under different machining conditions using an L_{27} orthogonal array from Taguchi. The results showed that a lower feed rate, higher speed and smaller drilling diameter minimize the pushing force. Nagamadhu et al. **[69]** conducted a study of delamination during drilling to different drill diameters of a composite sandwich reinforced vinyl ester with unidirectional sisal fibres using various cutting parameters. The authors used the Taguchi method L_9 to optimize the input parameters to minimize delamination. The researchers concluded that the optimal parameters of drill diameter, spindle speed and feed rate given by ANOVA were 6 mm, 3000 rpm and 50 mm/min, respectively. Machado et al. [62] proposed a new method for evaluating Fd (delamination factor). This technique is based on digital radiography image acquisition of the damaged area during drilling. In a recent work, Belaadi et al. **[32]** conducted an interesting investigation aimed at the effect of drilling parameters such as spindle speed, feed rate and drilling diameters on short jute fibre/polyester biocomposites to evaluate the effect of the delamination factor Fd. In other recent work, Belaadi et al. **[22]** developed an ANN model to assess the interactions of cutting parameters to analyse delamination. In their tests, hole exit damage was measured using a high-resolution scanner and then processed by ImageJ to calculate the delamination factor. The results revealed that delamination is sensitive to each cutting parameter.

Therefore, the novelty and innovation of this study consists of a focus on the influence of drilling machining parameters on the delamination factor (F_d) of biosandwich structures with agglomerated cork cores with epoxy skins reinforced with woven jute (WJF). Two tools with different diameters were chosen: conventional HSS-TiN (high-speed steel coated with titanium nitride) drills and wood drills (brad & spur), to estimate the influence and simultaneous interaction of the input parameters on the factor F_d. Indeed, response surface methodology (RSM) and artificial neural networks (ANNs) were utilized to estimate the influence and interaction of cutting parameters on output delamination in drilling. Finally, optimization functions such as desirability based on the RSM method, function *fmincon* and genetic algorithm (GA) were employed to confirm the optimal combination of optimal cutting parameters (f, N and d) in the biosandwich structures studied in this work.

2. Material And Methods

2.1. Biosandwich manufacturing

In this study, the reinforcement is composed of a bidirectional jute fibre (**Figure 1**) having a surface mass of 160 g/m^2 (28 x 23 yarns/100 mm) and an epoxy resin classified as MEDAPOXY STR, furnished by the GRANITEX company (Algeria), which has a density of 1.110 kg/m^3. The average tensile mechanical properties of epoxy resin used in this paper have been described by Belaadi et al. and Cherief et al. [22, 63] in previous work (tensile strength of 43.13 MPa, elongation of 4.03% and Young's modulus of 2.47 GPa). Additionally, materials were used as

agglomerate cores in the manufacturing of biosandwich samples as cork, with a thickness of 15 mm and a nominal density of 280 kg/m^3. The jute fabric, agglomerate cork and epoxy resin were procured from local sources. The preparation of the bio-sandwich samples (jute/cork/epoxy) was performed by a contact moulding process by hand and then cut to dimensions of 300×300 mm. The obtained sandwich structure was a rectangular sheet 300 mm long, 300 mm wide and approximately 20±0.8 mm thick and was made up of five layers. In addition, the biosandwich had a 30% fibre content by weight. The EBJWC assembly was cured and held in the mould at atmospheric standard pressure (1 bar) until curing was complete for 24 hours at an ambient temperature of 25°C. The plates were kept in open air for 15 to 20 days to ensure complete polymerization of the resin. Finally, they were then post-cured at 50°C for 8 hours in an oven. Following fabrication, the samples for drilling experiments were cut to the following dimensions: 290×100×20 mm^3. A diamond saw was used to cut the specimens, which were lubricated with water to avoid heating caused by the cutting process. The specimens were then air-dried at room temperature (25°C) for 20 days.

2.2. Drilling experimental procedure

The drilling tests were performed with a MOMAC universal drill using a 1400 rev/min spindle and a feed rate of 4.6 to 1040 mm/rev [22, 32], and all drilling was performed on this machine. To reduce the bending of the parts (and thus not include the influence of this structural parameter in this study) while drilling the hole, a solid steel support was used underneath the parts in the sandwich to avoid amplifying the size of the defect at the exit of the hole. To perform the drilling tests, we need a workpiece (EBJWC) size geometry of 290×100×20 mm^{3,} and a device for fixing the part is shown in **Figure 1**. Brad & spur and twist HSS-TiN drills of different diameters (5 mm, 7 mm and 10 mm) were used in this study, whose shape and tool geometry are presented in **Figure 1**. It is important to note that hole drilling in this study is performed in one phase (step). To obtain high-quality holes and prevent the drilling tool wear factor, the drill bit was replaced with a new bit after four to five operations. Drilling was done dry without coolant. In addition, other settings were also employed, such as 355, 710 and 1400 rpm spindle speeds and three feed rates that we chose (50, 108 and 190 mm/min). The selection of machining parameters was based on a literature review, which is presented in **Table 1**.

Next, drilled samples were digitally scanned with a high-resolution scanner at up to 2400 × 4800 dpi (48 bit internal colour depth) to obtain a high-quality image. Image digital results are imported into and processed in ImageJ (free software v1.47, published by the National Institute of Health, USA [37, 38, 64]) for damage area measurement of the drilled hole Fd, and the threshold factor was fitted to indicate delamination surrounding the hole. Delamination is a main damage defect in the drilling of laminated composites. The procedure used to acquire different damaged areas in a drilled hole is shown in **Figure 1**. The damage (delamination) was estimated in terms of the delamination factor (F_d). The delamination factor at exit was determined by the following equation:

$$F_d = \frac{D_{max}}{D} \qquad (1)$$

where D is the nominal diameter of the drilled hole, D_{max} is the maximum diameter of delamination and F_d is a conventional delamination factor.

An orthogonal array (L_{27}) of central composite design (CCD) was adopted as the experimental design in this study. It was selected to decrease the number of experiments. Therefore, the experimental cost and time were minimized.

For all three factors, namely, the drill diameter (*d*), spindle speed (*N*), and feed rate (*f*), three levels in each factor were envisaged in this study. **(Table 2)**.

3. Results And Discussion

3.1 Influence of the drilling parameters on the delamination factor

Figure 2 illustrates the condition of the holes drilled at the entrance and the exit (#4, #13 and #22) with feed rates of 50, 108 and 190 mm/min and a spindle speed of 355 rpm. Digital images of the machined biosandwich plates were taken with a resolution of 4800 pixels using a professional scanner. Two concentric circles were drawn using image processing software. The damage caused by drilling holes in the manufacture of biosandwiches is part of the delamination factor. This is conditioned by the choice of cutting parameters as well as by the fibre fabric used. Delamination is a fundamental concern for the choice of cutting parameters during the design process. Determination of the delamination factor F_d of biosandwich structures with agglomerated cork-core with epoxy skins reinforced with woven jute (EBJWC) for two drills using HSS-TiN and BSD is related to many factors such as feed rate, cutting speed and tool diameter.

3.2 Response surface methodology and ANOVA for delamination factor

The experimental results were processed using a response surface analysis and to determine the relationship between the delamination and different cutting parameters for HSS-TiN and BSD. **Table 3** shows the output parameters represented by the delamination factor for the two drills used in the present study, F_d(HSS-TiN) and F_d(BSD), performed under different machining conditions. These results were obtained according to the optimal design, which consists of analysing the influence of numerical factors on the responses with three levels and three input parameters (*f*, *N* et *d*). Indeed, response surface methodology (RSM) is a mathematical and statistical method that is generally used in applied science and analytical problems such as the mechanics and machining of materials **[65]**. In addition, this technique represents an empirical modelling approach with the objective of finding the relationship between the input and output parameters, that is, delamination F_d, by changing the different cutting parameters during the drilling of biosandwiches. The mathematical equations of the regression are presented in **Table 4** for the different delamination factors obtained by Design-Expert software, which recommended quadratic models. Quadratic regression models are second-order mathematical models based on the RSM. **Figures 3a** and **b** highlight the relationship of predicted and experimental results for biosandwich structure delamination of HSS-TiN and BSD drills. Thus, the results obtained show satisfactory agreement of the regression model since the predicted values are statistically identical to the experimental values with a confidence level of 95%. The normal probability curves of the delamination residues F_d are shown in **Figures 3c** and **d**; the straight lines reveal a good distribution of errors. The synthesis of the relevance of the results reveal that the quadratic model is statistically significant for the analysis of delamination. **Table 4** shows the results of the quadratic ANOVA model. The R^2 coefficient and the adjusted R^2 coefficient corresponding to the delamination are 87.59% and 81.02% for HSS-TiN and 89.35% and 83.71% for BSD, respectively. It is therefore obvious that this regression model offers a perfect match between the responses and the independent factors. The model is statistically significant because the p value corresponding to the model is less than 0.05. Additionally, factors *f* and *d* have significant effects on delamination. Due to the larger F_d value, it appears that the feed rate *f* and the diameter *d* are the most significant parameters for the delamination of HSS-TiN and BSD composites compared to *N*. The rest of the terms in the model are considered insignificant. Therefore, it appears that the feed rate is the main parameter that affects the delamination factor, followed by the

diameter and the cutting speed (*N*). In addition, the contribution of the factor f is the most important (66.04% and 66.03%) for HSS-TiN and BSD. The cutting speed has a less significant influence on delamination than the diameter on delamination.

3.3 3D surface plots for the delamination factor

Figures 4 and 5 describe a mapping in the form of the response surfaces provided for the delamination at the exit of the biosandwiches machined by the HSS-TiN and BSD drills as a function of the feed rate (*f*) and the cutting speed (*N*) and of the diameter (*d*). For the HSS-TiN tool, the delamination does not exceed 1.10 with a feed rate between 50 and 60 mm/min and a diameter of 5 to 7 mm, but further, the delamination exceeds 1.48 when the spindle speed is between 178 and 190 mm/min and a diameter of 9.4 to 10 mm (**Fig 4a**). For the BSD tool, we also notice that the delamination does not exceed 1.09 for feed rates between 50 and 70 mm/min and a diameter of 5 to 5.5 mm, but it exceeds 1.62 when the cutting speed is between 185 and 190 mm/min and a diameter of 7.8 to 10 mm (**Fig 5a**). **Figures 4b** and **5b** show how the feed rate and spindle speed significantly affect delamination for the HSS-TiN and BSD drills. It can be seen that the delamination increases significantly with increasing feed rate and very slightly with increasing spindle speed. For HSS-TiN and BSD, the delamination is less than 1.10 when the feed rate is between 50 and 64 mm/min and the cutting speed is between 355 and 1400 rpm and is 1.09 for BSD when the feed rate is between 50 and 75 mm/min and that *N* is between 562 and 1400 rev/min. The delamination also seems to rise above 1.32 for HSS-TiN when the feed rate is between 182 and 190 mm/min and *N* is between 510 and 1400 rpm and equals 1.43 for BSD when the feed rate is between 174 and 190 mm/min and the spindle speed is between 355 and 1400 rpm. This corresponds perfectly to the results obtained in the work of Belaadi et al. [22, 32] in the case of epoxy/jute fabric biocomposites for the same cutting conditions. The effect of drill bit diameter and cutting speed (*N*) on delamination is shown in **Figures 4c** and **5c**. From this figure, it appears that the delamination increases as the diameter increases and increases slightly with the increase of *N*. The delamination is less than 1.32 and 1.47, when the diameter of the tool (*d*) and cutting speed are between 5 and 5.8 mm and 355 and 484 rpm for the HSS-TiN tool and 5 and 5.7 mm and 355 and 1400 rpm for the BSD drill, respectively. In addition, it is also observed that F_d seems to exceed 1.52 and 1.62 when *d* and *N* are between 9.8-10 mm and 790-1400 rpm for HSS-TiN and 7.8-10 mm and 1295-1400 rpm for BSD, respectively. **Figure 6** presents the evolution of the delamination factor as a function of cutting parameters such as the feed rate (*f*), spindle speed (*N*) and diameter (*d*). The delamination factor increases with increasing feed rate and drill diameter, as shown in **Figure 6a**. The influence of these two cutting conditions (*f* and *d*) is also considerable; this is mainly due to the forces produced and the amount of material removed during machining. **Figure 6b** illustrates the effect of drill diameter and spindle speed on F_d for the two drills comprising HSS-TiN and BSD for a constant feed rate. The diameter of the drill has a great influence on the spindle speed, as clearly shown in **Figure 6b** for the first drill (HSS-TiN). In the event that the diameter of the drill bit is kept constant (**figure 6c**), the factor F_d increases with the increasing effect of the feed rate. On the other hand, by increasing the spindle speed, the delamination factor decreases. Generally, it emerges from **Figure 6** that the HSS-TiN drill (≈ 1.02 to 1.55) produces lower F_d values than the BSD drill (≈ 1.11 to 1.68).

3.4 Prediction of delamination factor by ANN model

The data were integrated into the network model by the input layer and the response by the output layer. A multilayer perceptron consisting of an input layer, a hidden layer and an output layer was used for the prediction of the delamination factor. The architecture design of the ANN network was designed using the MATLAB Neural Network Toolbox. Modelling by neural networks constitutes a powerful approach, making it possible to reproduce

the behaviour of any non-linear process of any kind [66]. For HSS-TiN and BSD drills, three neurons in the input layer, the hidden layers contain ten and twelve neurons, respectively, and one neuron for the output layer (**Figure 7)**. Determining the number of neurons in the hidden layers relies on reducing the error as the number of hidden nodes increases [67]**. Table 6** shows the tested ANN architectures and MSE and R values for training, validation and testing of Fd data for the HSS-TiN and BSD drill tools. These neurons are linked together by means of weight weights. In **Figures 8 a-c** and **8 d-f**, neural network prediction of F_d delamination and experimental test results for HSS-TiN and BSD tools, respectively, are compared for the training, testing and validation data sets. It emerges from **Figures 8** and **9** that the ANN prediction corresponds perfectly to the experimental results. The ANN models thus developed for HSS-TiN and BSD (**Table 7**) have the ability to interpret the data well and can serve as an efficient prediction tool for the delamination factor. In addition, the results show that the model is an efficient and applicable way to measure the delamination factor of biosandwiches made from jute fabric.

3.5 Comparison of RSM and ANN models

A comparison of the results predicted by the ANN and RSM models with those obtained experimentally are presented in **Figure 10**. It was found that the two models satisfactorily describe the results obtained experimentally. The maximum absolute percentage error in the prediction of the delamination factors of the HSS-TiN and BSD tools by the ANN model is 4.16% and 6.28%, respectively, while in the RSM model, this percentage is 6.93% and 7.78% (**Figure 9**). Thus, the ANN model provides a more accurate prediction than the RSM model. To the extent that these error rates are low, we can say that the optimization process is appropriate and that the model provides response prediction with high accuracy.

3.6 Optimisation of Responses

Figures 12 and **13** illustrate the distribution of the ramp function and the mapping of the desirability contour for the two types of drill material as well as their combination in **Figure 12c.** The main objective of the optimization is to determine the cutting parameters as well as the minimization of the delamination factors. The cutting parameters used in the optimization process are shown in **Table 8**, and the optimized values of the factors and responses are shown in **Table 9**. The ten runs are chosen due to the desirability factor near the unit. The first ten tests show that a high cutting speed and feed rate and a small tool diameter are suitable for reducing the delamination factor with desirability rates of 0.98 and 1.00 for HSS-TiN and BSD, respectively (**Figures 12a and b**). Indeed, according to the highest desirability value equal to 0.97, the optimal drilling machining conditions according to **Table 9** (f = 50 mm/min, N = 1399.99 rev/min and d = 5.61 mm) lead to minimal delamination (F_d) for HSS-TiN and BSD, whose values were 1.09 and 1.10, respectively.

The models obtained by the ANN method were retained for the resolution of the optimization problem using the genetic algorithm (GA) and for the search for the minimal multi-variable nonlinear constraint function (fmincon) using MATLAB software. **Table 10** shows the results obtained from the optimization of the input parameters and F_d for the two drill geometries (HSS-TiN and BSD). The results indeed reveal that the response of the GA and fmincon parameters provide approximately similar values. The results for comparison between the response parameters (*Fd*) obtained for the HSS-TiN and BSD tools with RSM and those predicted by the GA and fmincon algorithm are 1.08 and 1.03 obtained by RSM, 1.04 and 1.05 in the case of GA and 1.04 and 1.09 for the function *fmincon*, respectively, confirming the relevance of the models and the adequacy of the results with those obtained by [32].

4. Conclusion

The present research focused on the development and optimization of jute fibre polymer composite delamination factors with two types of HSS-TiN and BSD drills. The results obtained above showed following conclusions:

- Based on the effects of the combination of cutting parameters in the drilling process, a combination of a low feed rate and small tool diameter is clearly needed to minimize the delamination factor.
- The importance of the material and the feed rate in relation to the diameter of the drill are predominant on the delamination factor, and it has been noticed that spindle speed has no influence on the latter. The contribution of the different elements of the optimal drilling condition are as follows: feed rate (66.04%), drill diameter (10.54%) and spindle speed.
- The quality of the optimization is considered good with an overall desirability factor of 97%.
- The results of the predictive models and the experimental measurements are in good agreement.
- The average error percentages between the model and the experimental results are 0.26% for the HSS-TiN drill and 1.01% for the BSD drill.
- The ANN and RSM models applied to predict the cutting parameters in the drilling processes show very high agreement with the experimental data. The experimental results compared with those predicted by the RSM and ANN models indicate that ANN models are more accurate and produce excellent results.

Indeed, manufacturers seek to obtain better machinability of their products, regardless of the material. This detailed study will make it possible to choose the most appropriate machining conditions to obtain better machinability.

Declarations

Acknowledgements : The authors gratefully acknowledge (la Direction Générale de la Recherche Scientifique et du Développement Technologique, Algérie) DGRSDT for their support in this work.

Author contribution

Zohir Tabet : Conceptualization, Investigation, Methodology, Writing - review & editing.

Ahmed Belaadi: Conceptualization, Investigation, Methodology, Supervision, Writing - review & editing.

Messaouda Boumaaza: Conceptualization, Investigation, Writing - review & editing.

Mostefa Bourchak: Investigation, Writing - review & editing.

Funding information : The authors declare no funding information.

ORCID ID Ahmed Belaadi https://orcid.org/0000-0002-6059-3974

Data availability Not applicable.

COMPLIANCE WITH ETHICAL STANDARDS

Competing interests The authors declare no competing interests.

Ethics approval The work contains no libellous or unlawful statements, does not infringe on the rights of others, or contains material or instructions that might cause harm or injury.

Consent to participate The authors consent to participate.

Consent for publication The authors consent to publish.

References

1. Manaia JP, Manaia AT, Rodriges L (2019) Industrial Hemp Fibers: An Overview. Fibers 7
2. Koronis G, Silva A, Fontul M (2013) Green composites: A review of adequate materials for automotive applications. Compos Part B Eng 44:120–127. https://doi.org/https://doi.org/10.1016/j.compositesb.2012.07.004
3. Shahzad A (2011) Hemp fiber and its composites – a review. J Compos Mater 46:973–986. https://doi.org/10.1177/0021998311413623
4. Baley C, Le Duigou A, Bourmaud A, Davies P (2012) Influence of drying on the mechanical behaviour of flax fibres and their unidirectional composites. Compos Part A Appl Sci Manuf 43:1226–1233. https://doi.org/10.1016/j.compositesa.2012.03.005
5. Le Duigou A, Baley C (2014) Coupled micromechanical analysis and life cycle assessment as an integrated tool for natural fibre composites development. J Clean Prod 83:61–69. https://doi.org/10.1016/j.jclepro.2014.07.027
6. Diabor E, Funkenbusch P, Kaufmann EE (2019) Characterization of Cassava Fiber of Different Genotypes as a Potential Reinforcement Biomaterial for Possible Tissue Engineering Composite Scaffold Application. Fibers Polym 20:217–228. https://doi.org/10.1007/s12221-019-8702-9
7. Faruk O, Bledzki AK, Fink HP, Sain M (2012) Biocomposites reinforced with natural fibers: 2000-2010. Prog Polym Sci 37:1552–1596. https://doi.org/10.1016/j.progpolymsci.2012.04.003
8. amroune salah, Belaadi A, Bourchak M, et al Statistical and Experimental Analysis of The Mechanical Properties of Flax Fibers. J Nat Fibers. https://doi.org/10.1080/15440478.2020.1775751
9. Zhou Y, Fan M, Chen L (2016) Interface and bonding mechanisms of plant fibre composites: An overview. Elsevier Ltd
10. Rajmohan T, Vinayagamoorthy R, Mohan K (2019) Review on effect machining parameters on performance of natural fibre–reinforced composites (NFRCs). J Thermoplast Compos Mater 32:1282–1302. https://doi.org/10.1177/0892705718796541
11. Dutta S, Kim NK, Das R, Bhattacharyya D (2019) Effects of sample orientation on the fire reaction properties of natural fibre composites. Compos Part B Eng 157:195–206. https://doi.org/10.1016/j.compositesb.2018.08.118
12. Cherief M, Belaadi A, Bouakba M, et al (2020) Behaviour of lignocellulosic fibre-reinforced cellular core under low-velocity impact loading: Taguchi method. Int J Adv Manuf Technol. https://doi.org/10.1007/s00170-020-05393-9
13. Boumaaza M, Belaadi A, Bourchak M (2020) The Effect of Alkaline Treatment on Mechanical Performance of Natural Fibers-reinforced Plaster: Optimization Using RSM. J Nat Fibers. https://doi.org/10.1080/15440478.2020.1724236
14. Jaouadi M, M'sahli S, Sakli F (2009) Optimization and Characterization of Pulp Extracted from the Agave Americana L. Fibers. Text Res J 79:110–120. https://doi.org/10.1177/0040517508090781

15. Bedjaoui A, Belaadi A, Amroune S, Madi B (2019) Impact of surface treatment of flax fibers on tensile mechanical properties accompanied by a statistical study. Int J Integr Eng 6:10–17
16. Belaadi A, Amroune S, Bourchak M (2019) Effect of eco-friendly chemical sodium bicarbonate treatment on the mechanical properties of flax fibres: Weibull statistics. Int J Adv Manuf Technol. https://doi.org/10.1007/s00170-019-04628-8
17. Improving The Mechanical Performance of Biocomposite Plaster/ Washingtonian filifira Fibres Using the RSM Method. https://doi.org/10.1016/j.jobe.2020.101840
18. Weng B, Cheng D, Guo Y, et al (2020) Industrial Crops & Products Properties of Natural Lu ff a Vine as potential reinforcement for biomass composites. 155:
19. Engineering M, Ramzan M, Karim A, et al (2020) Sodium carbonate treatment of fibres to improve mechanical and water absorption characteristics of short bamboo natural fibres reinforced polyester composite composite. Plast Rubber Compos 0:1–9. https://doi.org/10.1080/14658011.2020.1768336
20. Malik K, Ahmad F, Gunister E (2021) Drilling Performance of Natural Fiber Reinforced Polymer Composites: A Review. J Nat Fibers 00:1–19. https://doi.org/10.1080/15440478.2020.1870624
21. Belaadi A, Laouici H, Bourchak M (2020) Mechanical and drilling performance of short jute fibre-reinforced polymer biocomposites: statistical approach. Int J Adv Manuf Technol 106:. https://doi.org/10.1007/s00170-019-04761-4
22. Belaadi A, Boumaaza M, Amroune S, Bourchak M (2020) Mechanical characterization and optimization of delamination factor in drilling bidirectional jute fibre-reinforced polymer biocomposites. Int J Adv Manuf Technol. https://doi.org/10.1007/s00170-020-06217-6
23. Rao YS, Mohan NS, Shetty N, Shivamurthy B (2019) Drilling and structural property study of multi-layered fiber and fabric reinforced polymer composite - a review. Mater Manuf Process 34:1549–1579. https://doi.org/10.1080/10426914.2019.1686522
24. Zhang H, Zhu P, Liu Z, et al (2020) Research on prediction method of mechanical properties of open-hole laminated plain woven CFRP composites considering drilling-induced delamination damage. Mech Adv Mater Struct 0:1–16. https://doi.org/10.1080/15376494.2020.1745969
25. Feito N, Díaz-Álvarez J, López-Puente J, Miguelez MH (2018) Experimental and numerical analysis of step drill bit performance when drilling woven CFRPs. Compos Struct 184:1147–1155. https://doi.org/10.1016/j.compstruct.2017.10.061
26. Fernández-Pérez J, Cantero JL, Díaz-Álvarez J, Miguélez MH (2017) Influence of cutting parameters on tool wear and hole quality in composite aerospace components drilling. Compos Struct 178:157–161. https://doi.org/10.1016/j.compstruct.2017.06.043
27. Feito N, Diaz-Álvarez J, López-Puente J, Miguelez MH (2016) Numerical analysis of the influence of tool wear and special cutting geometry when drilling woven CFRPs. Compos Struct 138:285–294. https://doi.org/10.1016/j.compstruct.2015.11.065
28. Feito N, Diaz-Álvarez A, Cantero JL, et al (2016) Experimental analysis of special tool geometries when drilling woven and multidirectional CFRPs. J Reinf Plast Compos 35:33–55. https://doi.org/10.1177/0731684415612931
29. Díaz-Álvarez J, Olmedo A, Santiuste C, Miguélez MH (2014) Theoretical estimation of thermal effects in drilling of woven carbon fiber composite. Materials (Basel) 7:4442–4454. https://doi.org/10.3390/ma7064442

30. Díaz-Álvarez A, Rodríguez-Millán M, Díaz-Álvarez J, Miguélez MH (2018) Experimental analysis of drilling induced damage in aramid composites. Compos Struct 202:1136–1144. https://doi.org/10.1016/j.compstruct.2018.05.068
31. Bayraktar Ş, Turgut Y (2020) Determination of delamination in drilling of carbon fiber reinforced carbon matrix composites/Al 6013-T651 stacks. Measurement 154:107493. https://doi.org/https://doi.org/10.1016/j.measurement.2020.107493
32. Belaadi A, Laouici H, Bourchak M (2020) Mechanical and drilling performance of short jute fibre-reinforced polymer biocomposites: statistical approach. Int J Adv Manuf Technol 106:1989–2006. https://doi.org/10.1007/s00170-019-04761-4
33. Chaitanya S, Singh I (2018) Ecofriendly treatment of aloe vera fibers for PLA based green composites. Int J Precis Eng Manuf - Green Technol 5:143–150. https://doi.org/10.1007/s40684-018-0015-8
34. De Olveira LÁ, Santos JC Dos, Panzera TH, et al (2018) Investigations on short coir fibre-reinforced composites via full factorial design. Polym Polym Compos 26:391–399. https://doi.org/10.1177/0967391118806144
35. Azuan SAS, Juraidi JM, Muhamad WMW (2012) Evaluation of Delamination in Drilling Rice Husk Reinforced Polyester Composites. Appl Mech Mater 232:106–110. https://doi.org/10.4028/www.scientific.net/AMM.232.106
36. Aravindh S, Umanath K (2015) Delamination in drilling of natural Fibre Reinforced Polymer Composites produced by Compression moulding. Appl Mech Mater 767:796–800. https://doi.org/10.4028/www.scientific.net/AMM.766-767.796
37. Sridharan V, Muthukrishnan N (2013) Optimization of machinability of polyester/modified jute fabric composite using grey relational analysis (GRA). Procedia Eng 64:1003–1012. https://doi.org/10.1016/j.proeng.2013.09.177
38. Sridharan V, Raja T, Muthukrishnan N (2016) Study of the Effect of Matrix , Fibre Treatment and Graphene on Delamination by Drilling Jute / Epoxy Nanohybrid Composite. Arab J Sci Eng 10–14. https://doi.org/10.1007/s13369-015-2005-2
39. Yallew TB, Kumar P, Singh I (2015) A study about hole making in woven jute fabric-reinforced polymer composites. Proc IMechE Part L J Mater Des Appl 0:1–11. https://doi.org/10.1177/1464420715587750
40. Monteiro SN, Terrones LAH, D'Almeida JRM (2008) Mechanical performance of coir fiber/polyester composites. Polym Test 27:591–595. https://doi.org/10.1016/j.polymertesting.2008.03.003
41. Jayabal S, Natarajan U (2011) Drilling analysis of coir – fibre-reinforced polyester composites. Bull Mater Sci 34:1563–1567. https://doi.org/doi.org/10.1007/s12034-011-0359-y
42. Bajpai PK, Singh I (2013) Drilling behavior of sisal fiber-reinforced polypropylene composite laminates. J Reinf Plast Compos 32:1569–1576. https://doi.org/10.1177/0731684413492866
43. Bajpai PK, Debnath K, Singh I (2015) Hole making in natural polylactic acid laminates : An experimental investigation. J Thermoplast Compos Mater 30:1–17. https://doi.org/10.1177/0892705715575094
44. Debnath K, Sisodia M, Kumar A, Singh I (2016) Damage-Free Hole Making in Fiber-Reinforced Composites: An Innovative Tool Design Approach. Mater Manuf Process 31:1400–1408. https://doi.org/10.1080/10426914.2016.1140191
45. Debnath K, Singh I, Dvivedi A (2014) Drilling Characteristics of Sisal Fiber-Reinforced Epoxy and Polypropylene Composites. Mater Manuf Process 29:1401–1409. https://doi.org/10.1080/10426914.2014.941870

46. Debnath K, Singh I, Dvivedi A (2017) On the analysis of force during secondary processing of natural fiber-reinforced composite laminates. Polym Compos 38:164–174. https://doi.org/10.1002/pc.23572
47. Chaudhary V, Gohil PP (2016) Investigations on Drilling of Bidirectional Cotton Polyester Composite. Mater Manuf Process 31:960–968. https://doi.org/10.1080/10426914.2015.1059444
48. Venkateshwaran N, ElayaPerumal A (2013) Hole quality evaluation of natural fiber composite using image analysis technique. J Reinf Plast Compos 32:1188–1197. https://doi.org/10.1177/0731684413486847
49. Athijayamani A, Thiruchitrambalam M, Natarajan U, Pazhanivel B (2010) Influence of alkali-treated fibers on the mechanical properties and machinability of roselle and sisal fiber hybrid polyester composite. Polym Compos 31:723–731. https://doi.org/10.1002/pc.20853
50. Ramesh M, Sri Ananda Atreya T, Aswin US, et al (2014) Processing and mechanical property evaluation of banana fiber reinforced polymer composites. Procedia Eng 97:563–572. https://doi.org/10.1016/j.proeng.2014.12.284
51. Ismail SO, Dhakal HN, Dimla E, et al (2016) Effects of drilling parameters and aspect ratios on delamination and surface roughness of lignocellulosic HFRP composite laminates. J Appl Polym Sci 133:. https://doi.org/10.1002/app.42879
52. Abilash N, Sivapragash M (2016) Optimizing the delamination failure in bamboo fiber reinforced polyester composite. J King Saud Univ - Eng Sci 28:92–102. https://doi.org/https://doi.org/10.1016/j.jksues.2013.09.004
53. Díaz-Álvarez A, Díaz-Álvarez J, Santiuste C, Miguélez MH (2019) Experimental and numerical analysis of the influence of drill point angle when drilling biocomposites. Compos Struct 209:700–709. https://doi.org/10.1016/j.compstruct.2018.11.018
54. Babu GD, Babu KS, Gowd BUM (2012) Effects of drilling parameters on delamination of hemp fiber reinforced composites. Int J Mech Eng Res Dev 2:1–8
55. Azuan SAS (2013) Effects of Drilling Parameters on Delamination of Coconut Meat Husk Reinforced Polyester Composites. Adv Environ Biol 7:1097–1100. https://doi.org/10.1007/978-3-642-38345-8_6
56. Roy Choudhury M, Srinivas MS, Debnath K (2018) Experimental investigations on drilling of lignocellulosic fiber reinforced composite laminates. J Manuf Process 34:51–61. https://doi.org/https://doi.org/10.1016/j.jmapro.2018.05.032
57. Durão LMP, Gonçalves DJS, Tavares JMRS, et al (2013) Drilling delamination outcomes on glass and sisal reinforced plastics. Mater Sci Forum 730–732:301–306. https://doi.org/10.4028/www.scientific.net/MSF.730-732.301
58. Chen W-C (1997) Some experimental investigations in the drilling of carbon fiber-reinforced plastic (CFRP) composite laminates. Int J Mach Tools Manuf 37:1097–1108. https://doi.org/https://doi.org/10.1016/S0890-6955(96)00095-8
59. Anand G, Alagumurthi N, Palanikumar K, et al (2018) Influence of drilling process parameters on hybrid vinyl ester composite. Mater Manuf Process 33:1299–1305. https://doi.org/10.1080/10426914.2018.1453161
60. Chandramohan D, Marimuthu K (2011) Drilling of Natural Fiber Particle Reinforced Polymer Composite Material. Int J Adv Eng Res Stud I:134–145
61. Mercy JL, Sivashankari P, Sangeetha M, et al (2020) Genetic Optimization of Machining Parameters Affecting Thrust Force during Drilling of Pineapple Fiber Composite Plates – an Experimental Approach. J Nat Fibers 1–12. https://doi.org/10.1080/15440478.2020.1788484

62. Machado CM, Silva D, Vidal C, et al (2021) A new approach to assess delamination in drilling carbon fibre-reinforced epoxy composite materials. Int J Adv Manuf Technol. https://doi.org/10.1007/s00170-021-06636-z
63. Cherief M, Belaadi A, Bouakba M, et al (2020) Behaviour of lignocellulosic fibre-reinforced cellular core under low-velocity impact loading: Taguchi method. Int J Adv Manuf Technol. https://doi.org/10.1007/s00170-020-05393-9
64. Davim JP, Rubio JC, Abrao AM (2007) A novel approach based on digital image analysis to evaluate the delamination factor after drilling composite laminates. Compos Sci Technol 67:1939–1945. https://doi.org/https://doi.org/10.1016/j.compscitech.2006.10.009
65. Majumder A (2010) COMPARISON OF ANN WITH RSM IN PREDICTING SURFACE ROUGHNESS WITH RESPECT TO PROCESS PARAMETERS IN Nd: YAG LASER DRILLING. Int J Eng Sci Technol 2:5175–5186
66. Karnik SR, Gaitonde VN, Davim JP (2008) A comparative study of the ANN and RSM modeling approaches for predicting burr size in drilling. Int J Adv Manuf Technol 38:868–883
67. Benardos PG, Vosniakos G-C (2003) Predicting surface roughness in machining: a review. Int J Mach Tools Manuf 43:833–844. https://doi.org/https://doi.org/10.1016/S0890-6955(03)00059-2
68. Rezghi Maleki H, Hamedi M, Kubouchi M, Arao Y (2019) Experimental study on drilling of jute fiber reinforced polymer composites. J Compos Mater 53:283–295
69. Ramesh M, Palanikumar K, Reddy KH (2014) Experimental investigation and analysis of machining characteristics in drilling hybrid glass-sisal-jute fiber reinforced polymer composites. In: 5th international & 26th all india manufacturing technology, design and research conference AIMTDR
70. Vinayagamoorthy R, Rajeswari N, Karthikeyan S (2015) Investigations of damages during drilling of natural sandwich composites. In: Applied Mechanics and Materials. Trans Tech Publ, pp 812–817
71. Vinayagamoorthy R, Rajeswari N, Sivanarasimha S, Balasubramanian K (2015) Fuzzy based optimization of thrust force and torque during drilling of natural hybrid composites. In: Applied Mechanics and Materials. Trans Tech Publ, pp 265–269
72. Ramnath BV, Sharavanan S, Jeykrishnan J (2017) Optimization of process parameters in drilling of fibre hybrid composite using Taguchi and grey relational analysis. In: IOP Conference Series: Materials Science and Engineering. IOP Publishing, p 12003
73. Vinayagamoorthy R (2017) Parametric optimization studies on drilling of sandwich composites using the Box–Behnken design. Mater Manuf Process 32:645–653. https://doi.org/10.1080/10426914.2016.1232811
74. Pailoor S, Murthy HNN, Sreenivasa TN (2021) Drilling of In-Line Compression Molded Jute / Polypropylene Composites. J Nat Fibers 18:91–104. https://doi.org/10.1080/15440478.2019.1612309
75. Çelik YH, Alp MS (2020) Determination of Milling Performance of Jute and Flax Fiber Reinforced Composites. J Nat Fibers 00:1–15. https://doi.org/10.1080/15440478.2020.1764435

Tables

Table 1: Process parameters available in open literature for drilling of jute fibre-reinforced polymer composites [22, 32, 72–75, 36–39, 68–71]

Matrix	Fibre	**Fibre content (% w/w)**	Cutting parameters				References
			Tool material	**Drill diameter d (mm)**	**Feed rate f (mm/rev)**	**Spindle Speed N (rpm)**	
Epoxy	Unidirectional Jute	-	HSS twist drills	6, 8, 10	50, 150, 250 (mm/min)	1000, 2000, 3000	[36]
Polyester	Treated and untreated Jute fabric	30	HSS twist drill	6	0.03, 0.06, 0.09, 0.12	9.42, 15.07, 20.72, 26.36 (m/min)	[37]
Epoxy and Polyester	Treated and untreated Jute fabric	30	HSS twist drill	6	0.03, 0.06, 0.09, 0.12	500, 800, 1100, 1400	[38]
Polypropylene (PP)	Jute fabric	30, 40, 50	Twist drills Jo drills, parabolic drills	8	0.05, 0.12, 0.19	900, 1800 2800	[39]
Epoxy	Jute fabric	43	HSS twist drill CoroDrill 854, N_2OC CoroDrill 856, N_2OC	8	0.05, 0.10, 0.15	750, 1250, 1750	[68]
Polyester	Glass-sisal-jute	-	Brad & Spur, coated carbide	6, 9, 12	0.04, 0.06, 0.08	1000, 2000, 3000	[69]
Vinyl-ester	Untreated Vetiver- jute-glass	-	Twist drills, 60°, 90°,120°, 150°	10	0.1, 0.2, 0.3, 0.4	500, 1000, 1500, 2000	[70]
Vinyl-ester	Treated (NaOH) Vetiver- jute-glass	-	Twist drills, 60°, 90°,120°, 150°	10	0.1, 0.2, 0.3, 0.4	500, 1000, 1500, 2000	[71]
Epoxy	Glass-flax-jute		Drill bit carbide	6, 8, 10	0.1, 0.2, 0.3	600, 1200 1800	[72]
Polyester	Short jute fibre 5, 10 and 15 mm	40	Brad & Spur drills Twist drills	5, 7, 10	50, 108, 190 (mm/min)	355, 710, 1400	[32]

Epoxy	Jute fabric (210 g/m^2)	40	Brad & Spur drills Twist drills (HSS) Twist drills (HSS-TiN)	5, 7, 10	50, 108, 190 (mm/min)	355, 710, 1400	[22]
Polyester	Jute fabric and steel fibres		HSS, 90°,120°,150°	8,10,12	0.1, 0.2, 0.3	500, 1250, 2000	[73]
Polypropylene	Unidirectional Jute	30	HSS, Co-HSS	2, 3, 4	0.1, 0.2, 0.3	600, 1260 2700	[74]
Epoxy	Jute and flax fabric	-	HSS, HSS-TiN, WC	4	0.01, 0.015, 0.020	2500, 5000, 7500	[75]
Epoxy	**Jute fabric (160 g/m^2) and cork**	**30**	**Brad & Spur drills and Twist drills (HSS-TiN)**	**5, 7, 10**	**50, 108, 190 (mm/min)**	**355, 710, 1400**	**This work**

Table 2. Design of experiments.

n°	Factors	Notation	Unite	Levels		
				-1	0	+1
				lowest	central	highest
1	Spindle speed	*N*	rev/min	355	710	1400
2	Feed rate	*f*	mm/min	50	108	190
3	Drill diameter	*d*	mm	5	7	10

Table 3. Experimental results for delamination factor of the drilled holes at the exit.

Test number	Input variables			Output variables					
	f (mm/min)	N (rev/min)	d (mm)	$F_{d(\text{HSS-TiN})}$			$F_{d(\text{BSD})}$		
				EXP	RSM	ANN	EXP	RSM	ANN
1	50	355	5	1.084	1.087	1.121	1.132	1.154	1.097
2	108	355	5	1.176	1.152	1.190	1.194	1.287	1.211
3	190	355	5	1.312	1.309	1.299	1.485	1.468	1.433
4	50	710	5	1.025	1.107	1.053	1.113	1.051	1.053
5	108	710	5	1.218	1.173	1.229	1.221	1.193	1.166
6	190	710	5	1.334	1.333	1.334	1.358	1.387	1.351
7	50	1400	5	1.045	1.092	1.029	1.117	1.034	1.094
8	108	1400	5	1.201	1.163	1.221	1.141	1.195	1.328
9	190	1400	5	1.355	1.328	1.344	1.423	1.416	1.640
10	50	355	7	1.127	1.086	1.113	1.306	1.280	1.147
11	108	355	7	1.181	1.168	1.193	1.413	1.412	1.361
12	190	355	7	1.321	1.350	1.313	1.678	1.591	1.573
13	50	710	7	1.117	1.109	1.101	1.121	1.194	1.143
14	108	710	7	1.217	1.193	1.274	1.429	1.335	1.392
15	190	710	7	1.320	1.377	1.319	1.479	1.528	1.498
16	50	1400	7	1.119	1.100	1.108	1.102	1.211	1.065
17	108	1400	7	1.246	1.188	1.248	1.387	1.370	1.347
18	190	1400	7	1.302	1.378	1.319	1.594	1.589	1.634
19	50	355	10	1.136	1.161	1.134	1.199	1.256	1.241
20	108	355	10	1.206	1.270	1.219	1.431	1.386	1.361
21	190	355	10	1.464	1.488	1.419	1.559	1.563	1.595
22	50	710	10	1.298	1.188	1.241	1.277	1.196	1.225
23	108	710	10	1.279	1.298	1.276	1.301	1.335	1.339
24	190	710	10	1.481	1.520	1.487	1.443	1.525	1.603
25	50	1400	10	1.171	1.188	1.194	1.272	1.263	1.199
26	108	1400	10	1.275	1.302	1.200	1.414	1.420	1.366
27	190	1400	10	1.555	1.529	1.546	1.684	1.637	1.577

Table 4. Mathematical models for delamination factor for drilling of jute fabric-cork /epoxy biosandwich structure obtained with RSM method.

RSM response	Drill geometry
	HSS-TiN
F_d	$1.252 - 0.579 \times 10^{-3} \times f + 0.106 \times 10^{-3} \times N - 0.070 \times d + 1.016 \times 10^{-7} \times f \times N + 1.504 \times 10^{-4} \times f \times d + 4.110 \times 10^{-6} \times N \times d + 5.725 \times 10^{-6} \times f^2 - 7.276 \times 10^{-8} \times N^2 + 0.005 \times d^2$
	BSD
F_d	$+0.442 + 2.258 \times 10^{-3} \times f - 0.709 \times 10^{-3} \times N + 0.225 \times d + 4.631 \times 10^{-7} \times f \times N - 1.100 \times 10^{-5} \times f \times d + 2.425 \times 10^{-5} \times N \times d - 5.286 \times 10^{-7} \times f^2 + 2.565 \times 10^{-7} \times N^2 - 0.014 \times d^2$

Table 5. ANOVA for the response surface quadratic model for delamination factor

Source	DF	SS	MS	F-value	P-value	Cont. %	Remarks
a) ANOVA for delamination factor of HSS-TiN							
Model	9	0.47	0.052	13.34	< 0.0001		Significant
f	1	*0.35*	*0.35*	*89.92*	*< 0.0001*	66.04	Significant
N	1	*2.338E-003*	*2.338E-003*	*0.60*	*0.4483*	0.30	
d	1	*0.083*	*0.083*	*21.47*	*0.0002*	10.54	Significant
f× *N*	1	*1.732E-004*	*1.732E-004*	*0.045*	*0.8352*	0.02	
f×*d*	1	*8.508E-003*	*8.508E-003*	*2.19*	*0.1570*	1.08	
N×*d*	1	*3.626E-004*	*3.626E-004*	*0.093*	*0.7635*	0.05	
f×*f*	1	*4.405E-003*	*4.405E-003*	*1.14*	*0.3016*	0.56	
N×*N*	1	*1.843E-003*	*1.843E-003*	*0.47*	*0.5000*	0.23	
d×*d*	1	*5.568E-003*	*5.568E-003*	*1.43*	*0.2474*	0.71	
Error	17	0.066	3.880E-003				
Total	26	0.53					
SD= 0.062 Mean = 1.245 Coefficient of variation = 4.999% Predicted residual error of sum of squares (PRESS) = 0.156						R^2= 87.59% R^2 adjusted = 81.02% R^2 predicted = 70.51% Adequate precision = 11.681	
c) ANOVA for delamination factor of BSD							
Model	9	0.7036	0.0782	15.8494	0.0000		Significant
f	1	0.5200	0.5200	105.4197	0.0000	66.03	Significant
N	1	0.0024	0.0024	0.4799	0.4978	0.30	
d	1	0.1152	0.1152	23.3487	0.0002	14.63	Significant
f× *N*	1	0.0036	0.0036	0.7290	0.4051	0.46	
f×*d*	1	0.0000	0.0000	0.0092	0.9246	0.00	
N×*d*	1	0.0126	0.0126	2.5587	0.1281	1.60	
f×*f*	1	0.0000	0.0000	0.0076	0.9315	0.00	
N×*N*	1	0.0229	0.0229	4.6458	0.0458	2.91	
d×*d*	1	0.0430	0.0430	8.7090	0.0089	5.46	
Error	17	0.0839	0.0049				
Total	26	0.7875					
SD= 0.070							

Mean = 1.343

Coefficient of variation = 5.23%

Predicted residual error of sum of squares (PRESS) = 0.208

R^2= 89.35%

R^2 adjusted = 83.71%

R^2 predicted = 73.49%

Adequate precision = 14.101

Table 6 ANN and MSE and R values architectures for training, validation and testing for HSS-TiN and BSD tools.

Model	Network Structure		Percentage	Samples	RMSE	R value
$F_{d(\text{HSS-TiN})}$	3-10-1	Training	85	22	1.55738E-4	9.95854E-4
		Validation	5	1	7.09654E-5	0.00000E-0
		Testing	15	4	3.34586E-4	9.99250E-4
$F_{d(\text{BSD})}$	3-12-1	Training	70	19	4.89445E-3	9.33291E-1
		Validation	4	4	2.14720E-2	8.00842E-1
		Testing	4	4	4.26253E-3	9.90948E-1

Table 7. Mathematical models for F_d *for drilling of jute fabric-cork /epoxy biosandwich structure obtained with ANN method.*

ANN response	Drill geometry
	HSS-TiN
F_d	$1.1311 + 0.0657 \times H_1 - 0.3190 \times H_2 - 0.0701 \times H_3 - 0.1217 \times H_4 - 0.1666 \times H_5 - 0.0713 \times H_6 + 0.0514 \times H_7 + 0.0852 \times H_8 + 0.0594 \times H_9 + 0.0596 \times H_{10}$
	$H_1 = \tanh(0.5 \times (-0.0014 \times f + 0.0028 \times N + 0.4176 \times d - 5.7214))$
	$H_2 = \tanh(0.5 \times (-0.0058 \times f - 0.0001 \times N + 0.1945 \times d - 2.0769))$
	$H_3 = \tanh(0.5 \times (0.0307 \times f - 0.0011 \times N - 0.5380 \times d + 0.0155))$
	$H_4 = \tanh(0.5 \times (-0.0115 \times f + 0.0011 \times N - 0.5036 \times d + 5.5530))$
	$H_5 = \tanh(0.5 \times (-0.0160 \times f + 0.0010 \times N + 0.15627 \times d + 0.3691))$
	$H_6 = \tanh(0.5 \times (-0.0277 \times f - 0.0018 \times N + 0.1578 \times d + 4.2872))$
	$H_7 = \tanh(0.5 \times (-0.0205 \times f + 0.0026 \times N - 0.7482 \times d + 7.7941))$
	$H_8 = \tanh(0.5 \times (0.0088 \times f - 0.0023 \times N + 0.2148 \times d + 0.4729))$
	$H_9 = \tanh(0.5 \times (-0.0145 \times f + 0.0005 \times N + 0.6481 \times d - 4.9045))$
	$H_{10} = \tanh(0.5 \times (0.0002 \times f + 0.0003 \times N + 0.4914 \times d - 4.5155))$
	BSD
F_d	$1.3203 - 1.630 \times H_1 + 1.4059 \times H_2 + 0.4465 \times H_3 + 0.9034 \times H_4 + 0.0229 \times H_5 - 0.8512 \times H_6 + 0.0710 \times H_7 - 0.6178 \times H_8 + 0.20575 \times H_9 + 0.6614 \times H_{10} + 0.9535 \times H_{11} + 0.4120 \times H_{12}$
	$H_1 = \tanh(0.5 \times (0.2113 - 0.0010 \times f + -0.0000 \times N - 0.01422 \times d))$
	$H_2 = \tanh(0.5 \times (-0.1455 + 0.0008 \times f + -0.0000 \times N + 0.0080 \times d))$
	$H_3 = \tanh(0.5 \times (-0.0393 + 0.0002 \times f - 0.0000 \times N + 0.0024 \times d))$
	$H_4 = \tanh(0.5 \times (-0.0819 + 0.0005 \times f - 0.0000 \times N + 0.0038 \times d))$
	$H_5 = \tanh(0.5 \times (-0.0004 + 0.0000 \times f - 0.0000 \times N - 0.0002 \times d))$
	$H_6 = \tanh(0.5 \times (0.0587 - 0.0004 \times f + 0.0000 \times N - 0.0021 \times d))$
	$H_7 = \tanh(0.5 \times (-0.0033 + 0.0000 \times f + 0.0000 \times N - 0.0003 \times d))$
	$H_8 = \tanh(0.5 \times (0.0538 - 0.0003 \times f + 0.0000 \times N - 0.0031 \times d))$
	$H_9 = \tanh(0.5 \times (-0.0153 + 0.0001 \times f + 0.0000 \times N + 0.0005 \times d))$
	$H_{10} = \tanh(0.5 \times (-0.0554 + 0.0003 \times f - 0.0000 \times N + 0.0022 \times d))$
	$H_{11} = \tanh(0.5 \times (-0.0851 + 0.0005 \times f - 0.0000 \times N + 0.0042 \times d))$
	$H_{12} = \tanh(0.5 \times (-0.0344 + 0.0002 \times f - 0.0000 \times N + 0.0015 \times d))$

Table 8. Goals and parameter ranges for RSM optimization of cutting conditions.

Condition	Goal	Lower limit	Upper limit
Feed rate, *f* (mm/min)	Is in range	50	190
Spindle speed, *N* (rev/min)	Is in range	355	1400
Drill, d (mm)	Is in range	5	10
$F_{d(\text{HSS-TiN})}$	Minimize	1.025	1.581
$F_{d(\text{BSD})}$	Minimize	1.102	1.684

Table 9. Response optimization for response parameters using RSM.

Test n°	Machining parameters			Response parameters		Desirability
	f (mm/min)	*N* (rev/min)	*d* (mm)	$F_{d(\text{HSS-TiN})}$	$F_{d(\text{BSD})}$	
1	50.000	1399.987	5.607	1.090	1.100	0.969
2	50.006	1399.971	5.629	1.090	1.102	0.969
3	50.000	1399.992	5.579	1.090	1.097	0.969
4	50.001	1399.999	5.508	1.090	1.090	0.969
5	50.001	1399.982	5.312	1.091	1.069	0.969
6	50.553	1400.000	5.610	1.091	1.101	0.969
7	50.000	1399.645	5.226	1.091	1.060	0.969
8	50.001	1399.989	5.146	1.091	1.051	0.969
9	50.000	1394.381	5.225	1.091	1.059	0.969
10	50.001	1399.983	5.085	1.092	1.044	0.969

Table 10. Comparing the response optimization techniques RSM, GA and fmincon optimization

Machining parameters			Response parameters	
f (mm/min)	*N* (rev/min)	*d* (mm)	F_d	Tools
RSM optimization				
50.000	355.002	6.047	1.0822	HSS-TiN
57.029	1023.600	5.034	1.0351	BSD
GA optimization				
51.162	1397.54	5.981	1.0401	HSS-TiN
51.091	1378.07	5.960	1.0489	BSD
fmincon optimization				
50.979	1397.52	5.992	1.0404	HSS-TiN
51.109	1391.06	6.012	1.0942	BSD

Figures

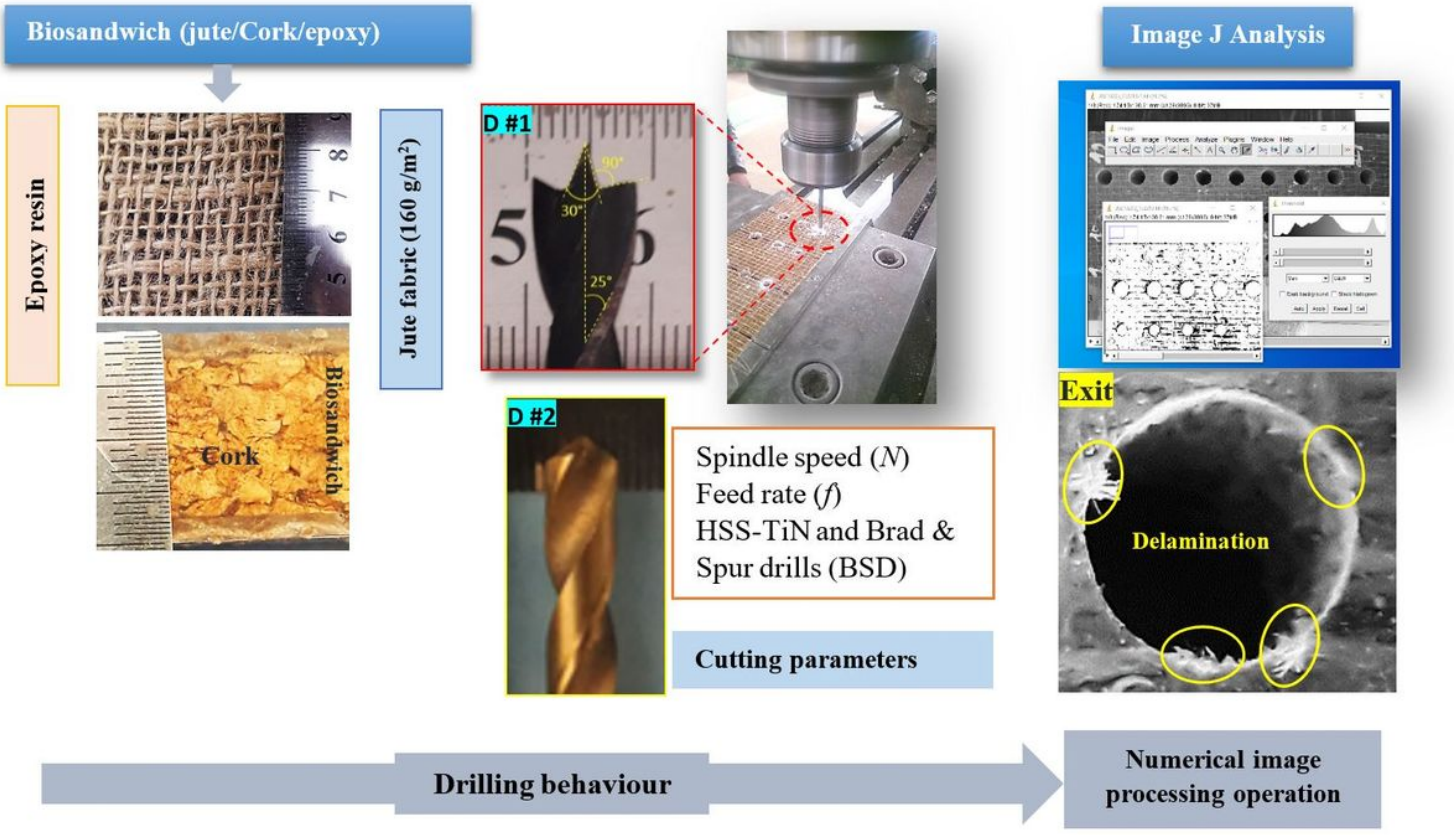

Figure 1

Schematic arrangement of experimental setup of the biosandwich structure.

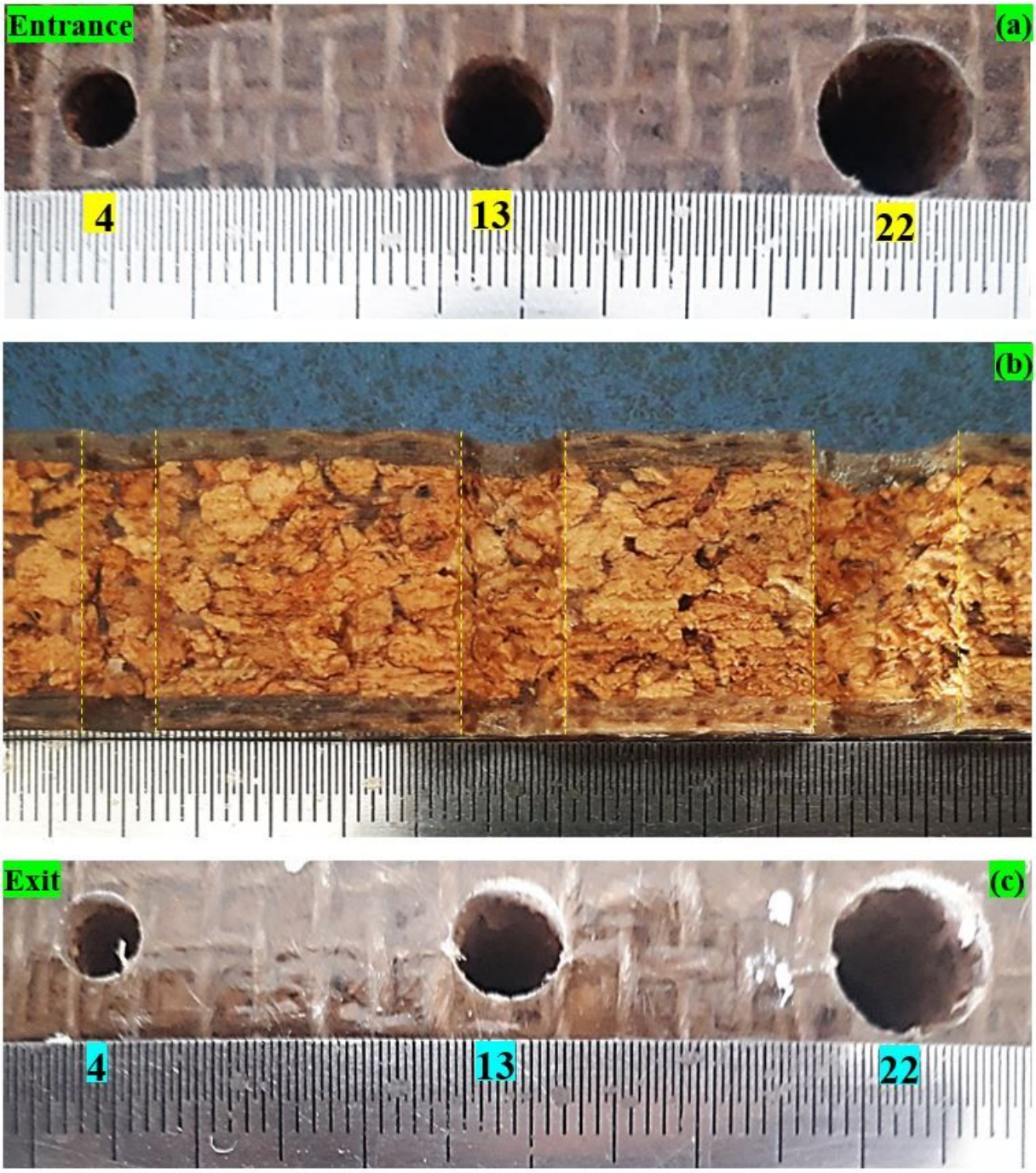

Figure 2

Typical holes drilled on jute/cork/epoxy biosandwich plate (a) entrance (b) cross section and (c) exit delamination for three test (#4, #13 and #22).

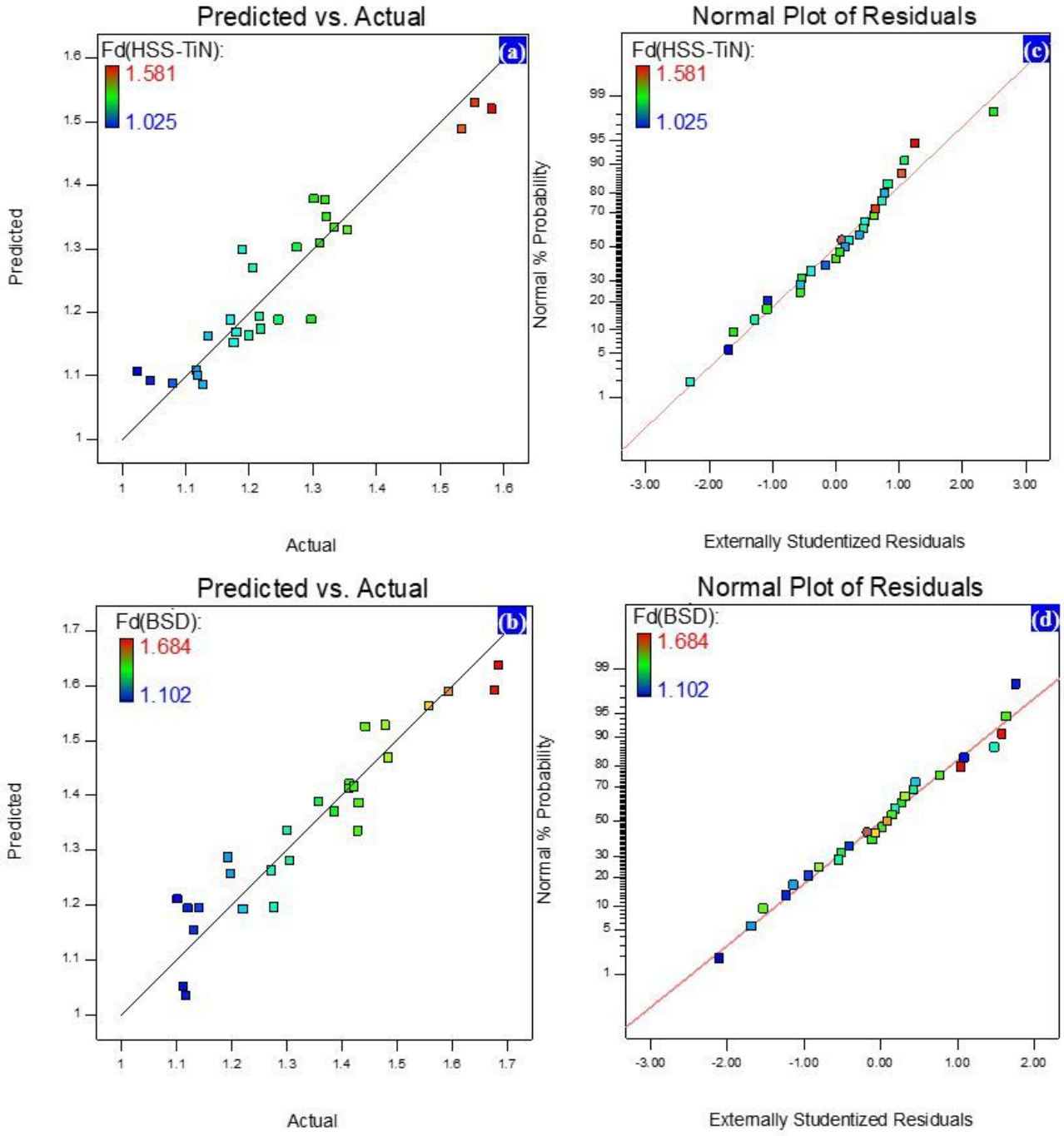

Figure 3

(a,b) Predicted vs. actual values and (c,d) Normal probability distribution of the Fd residuals for different drills used in this work.

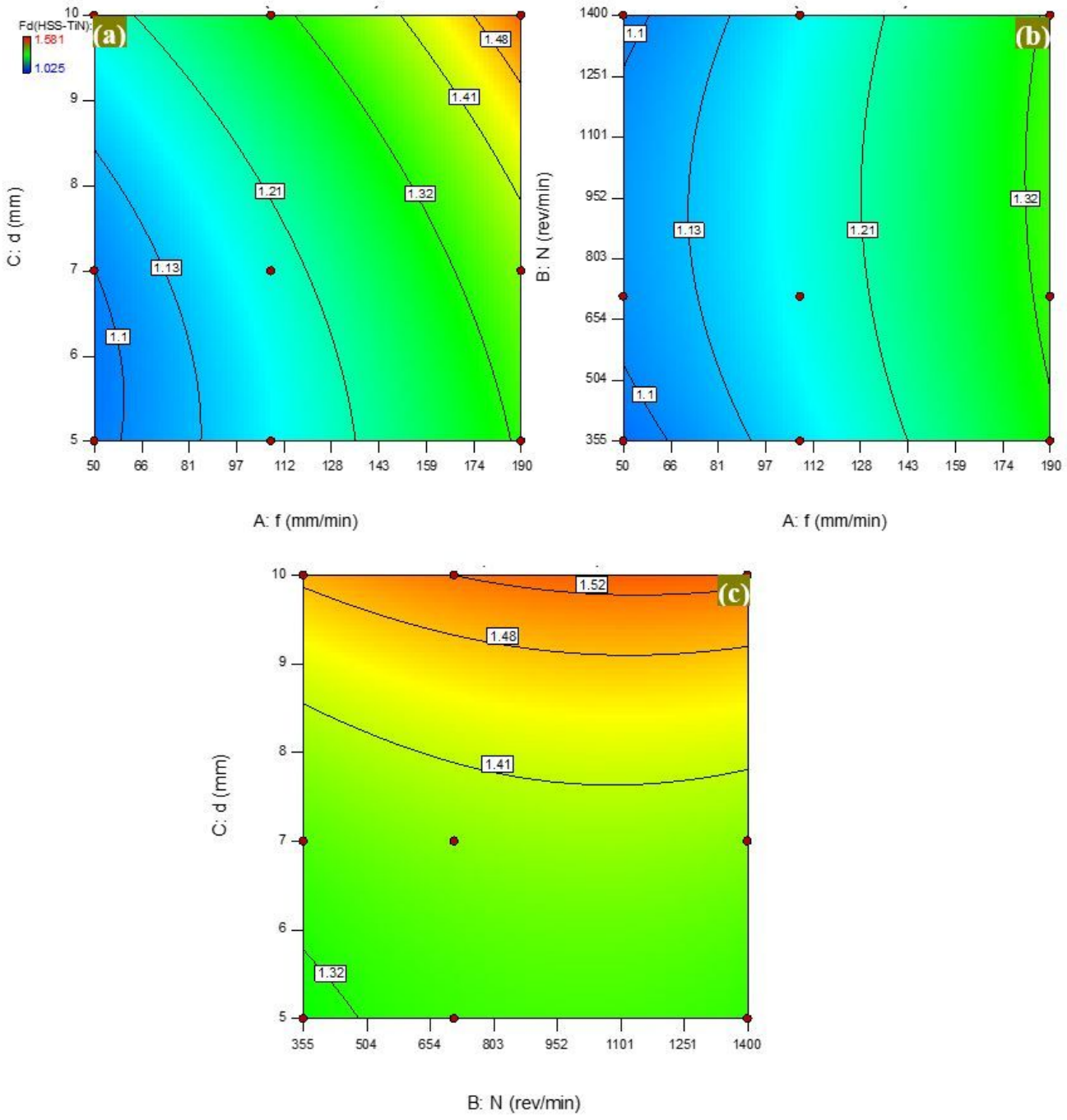

Figure 4

Representation of the response surfaces of the Fd data with HSS-TiN drill: (a) Feed rate vr. drill diameter, (b) Feed rate vr. spindle speed, (c) Spindle speed vr. drill diameter.

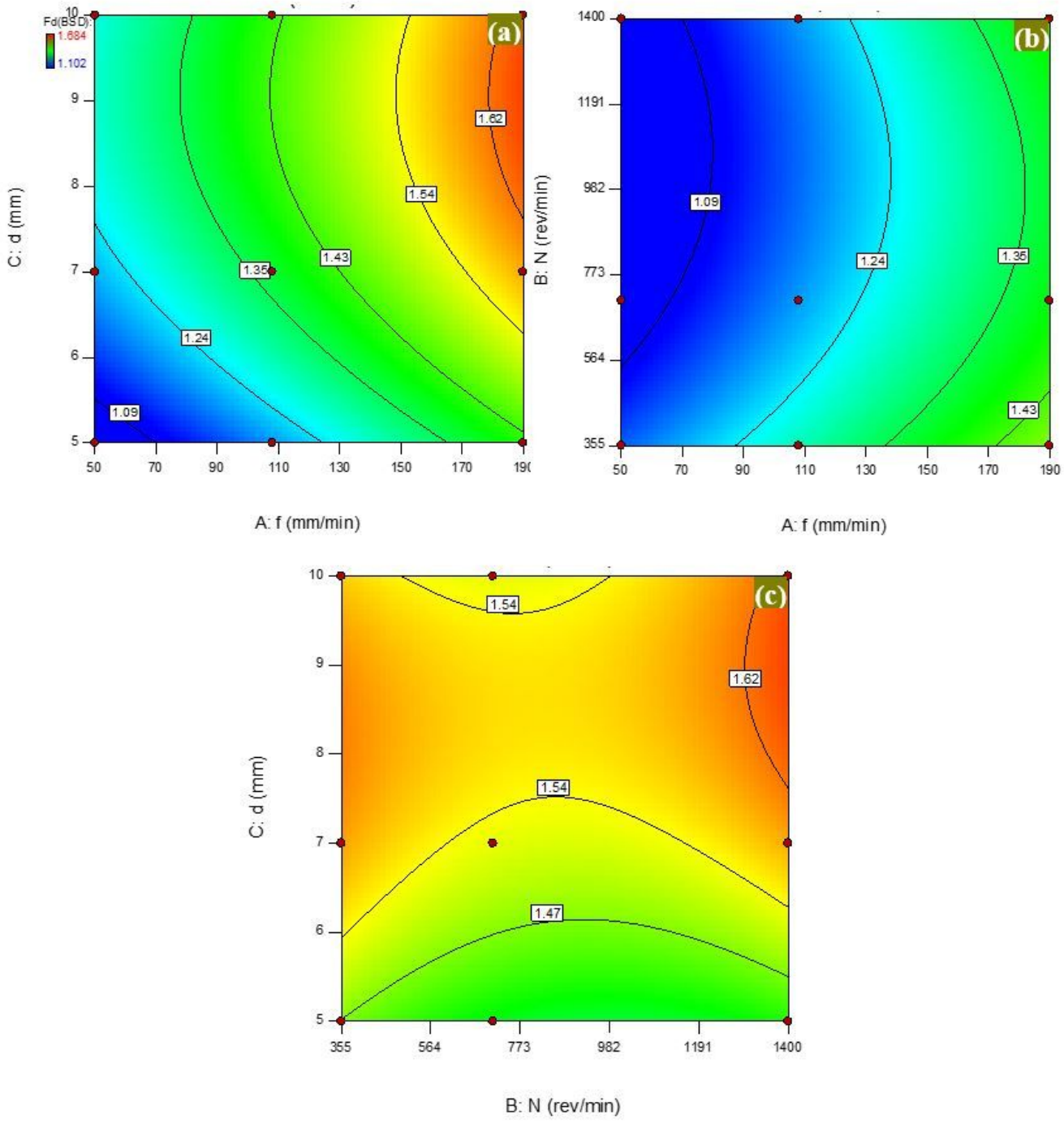

Figure 5

Representation of the response surfaces of the Fd data with BSD drill: (a) Feed rate vr. drill diameter, (b) Feed rate vr. spindle speed, (c) Spindle speed vr. drill diameter.

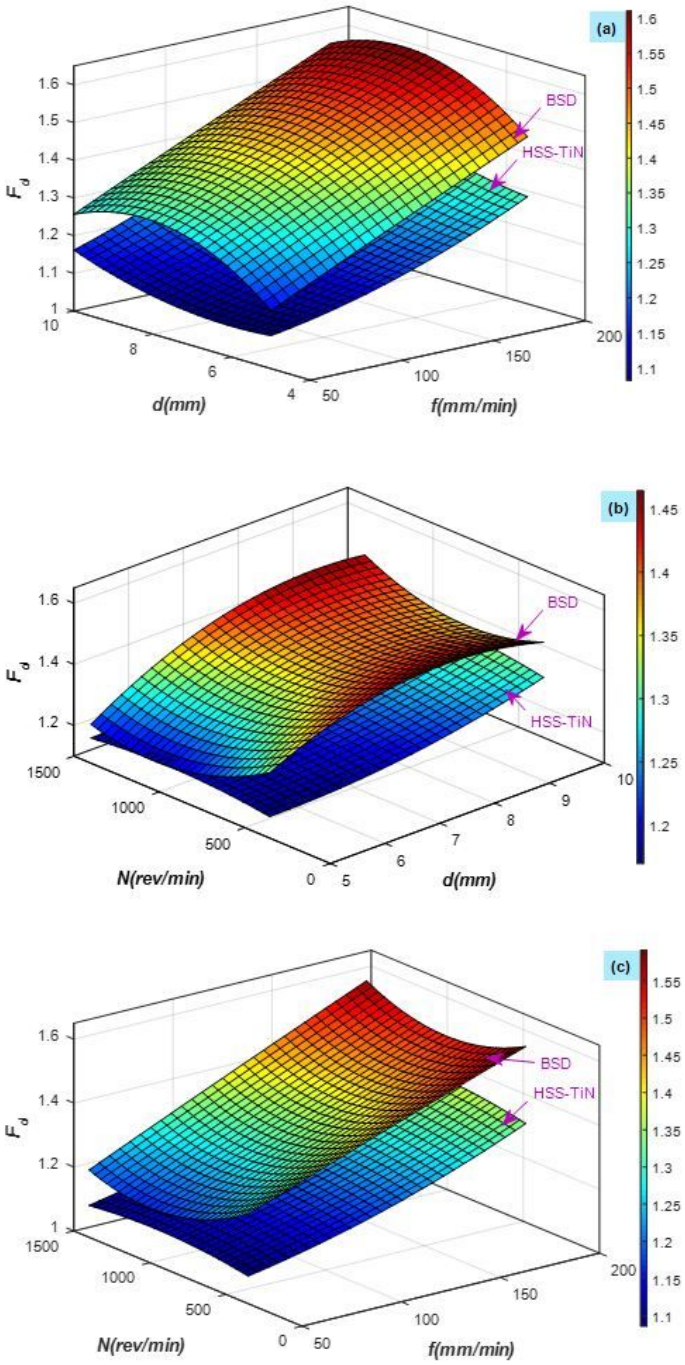

Figure 6

3D surface plots of delamination factor versus f, N and d of biosandwichs structures.

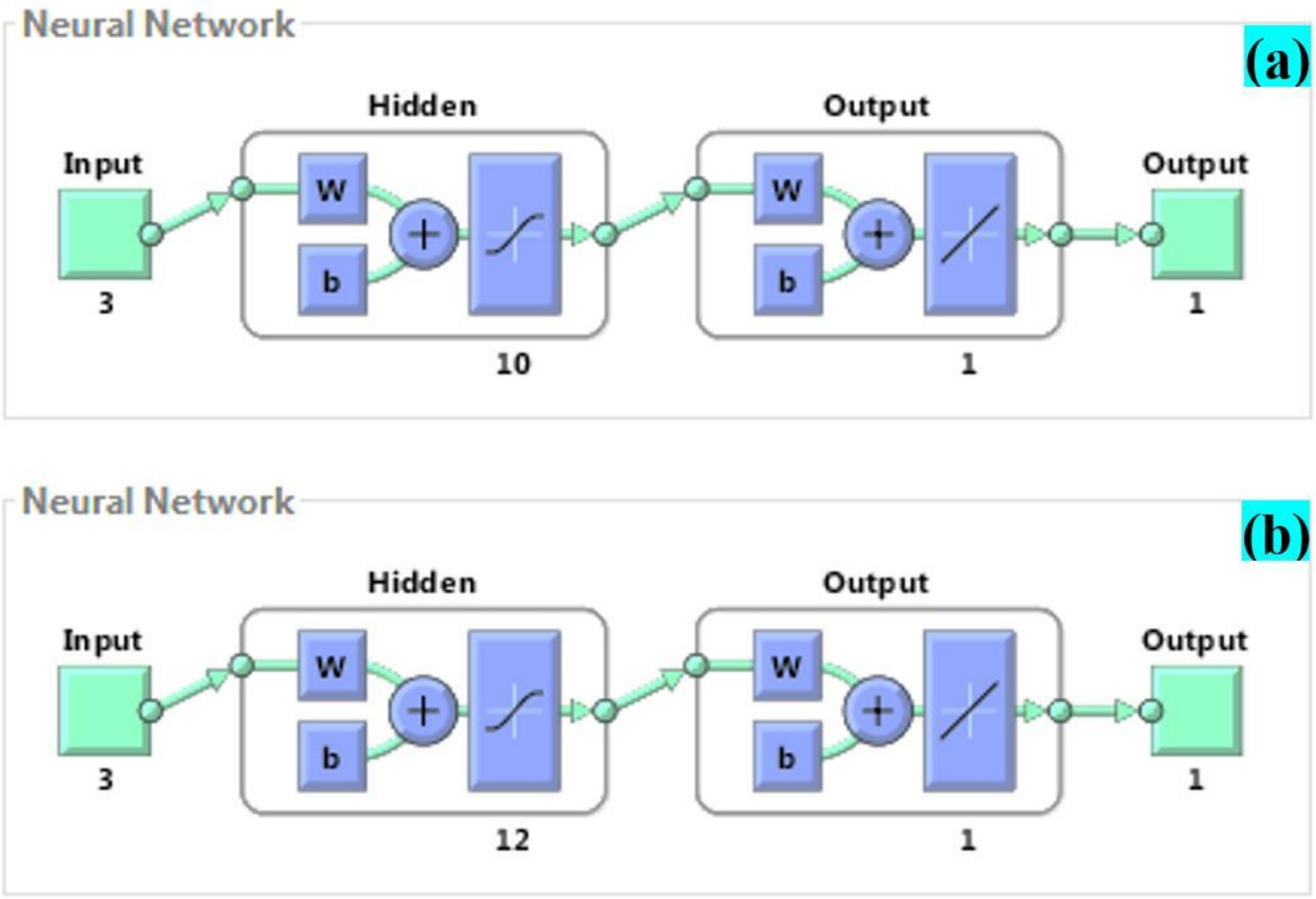

Figure 7

ANN architecture used for (a) HSS-TiN and (b) BSD tool.

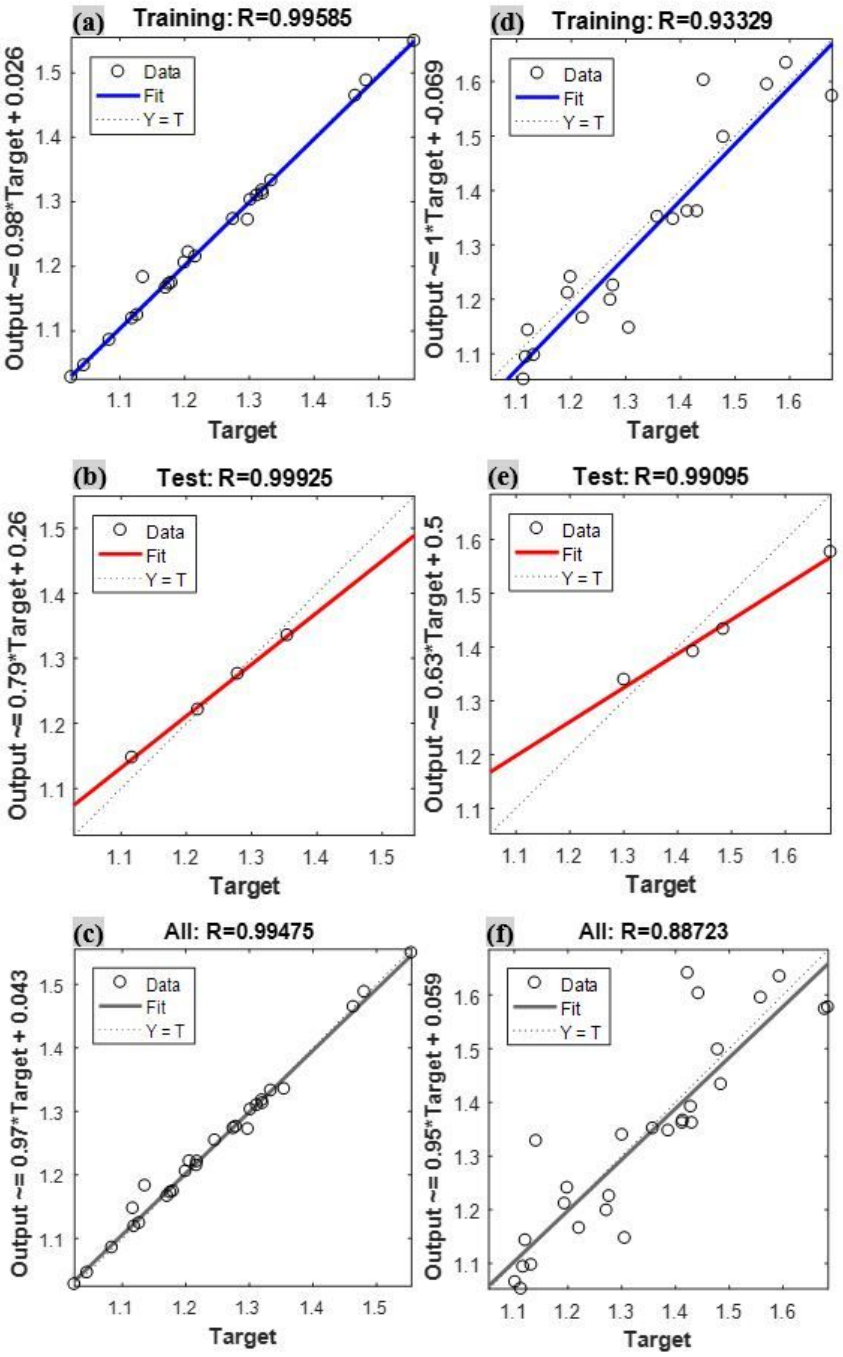

Figure 8

Regression validation scheme of Fd data (a-c) HSS-TiN and (e-f) BSD tools.

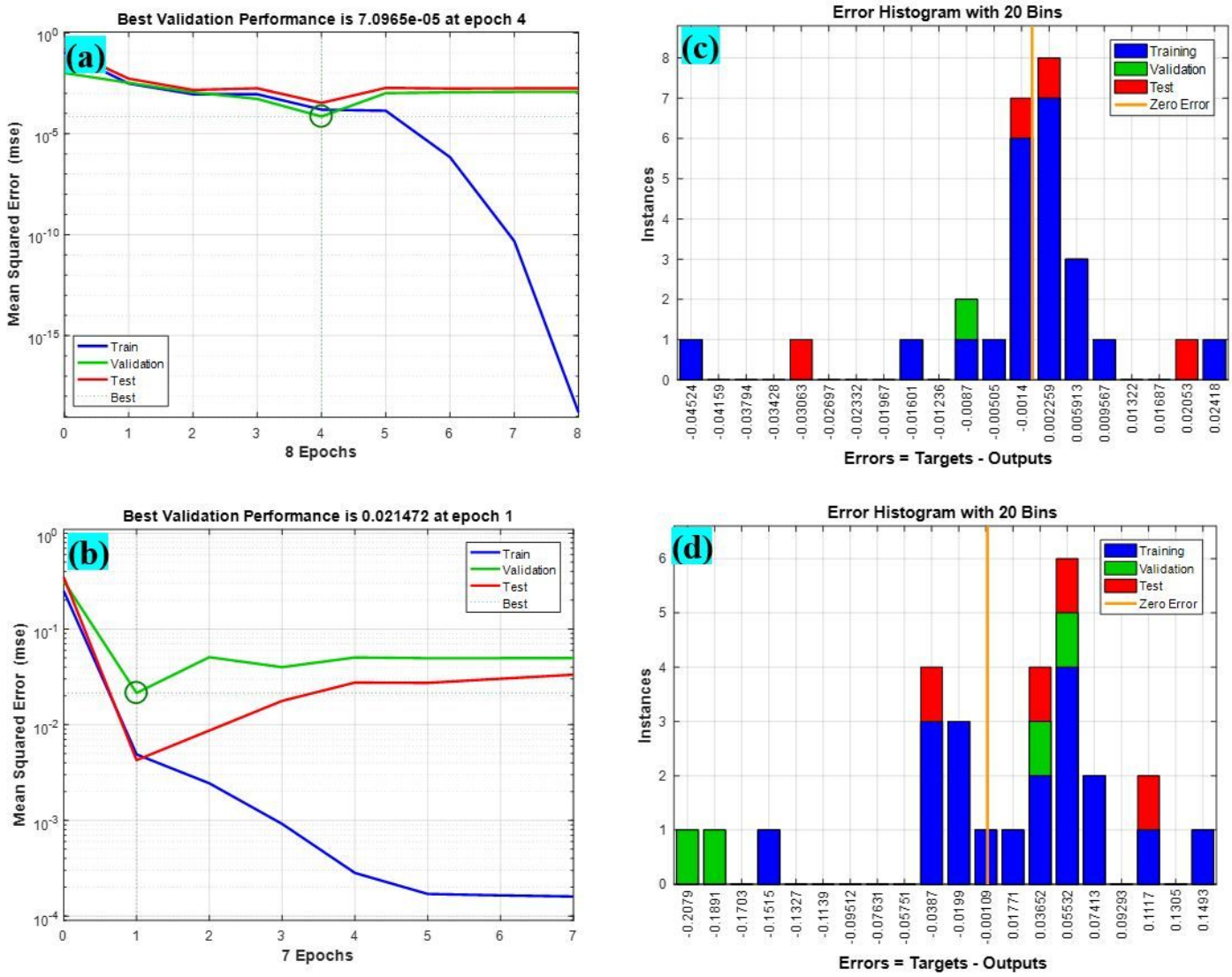

Figure 9

ANN validation results (a,b) HSS-TiN and (c,d) BSD tools.

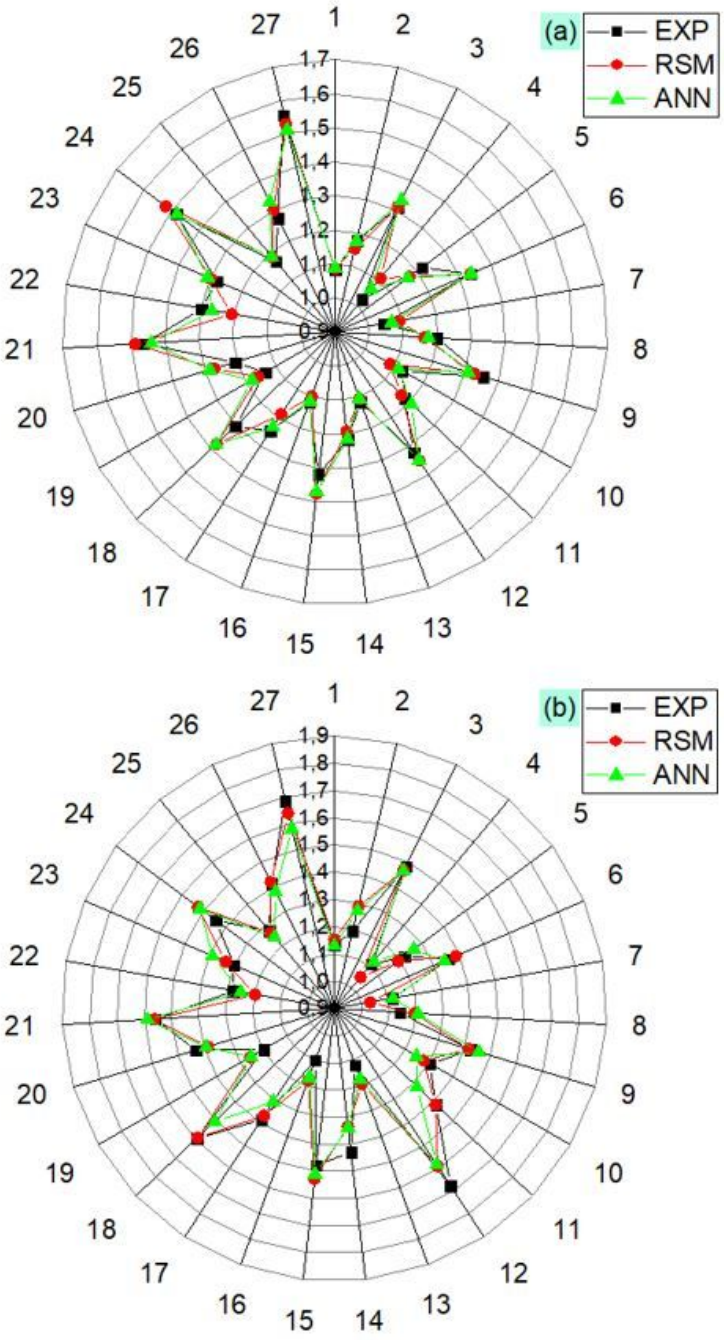

Figure 10

Comparison between experimental and predicted Fd with RSM and ANN models (a) HSS-TiN and (c) BSD drills.

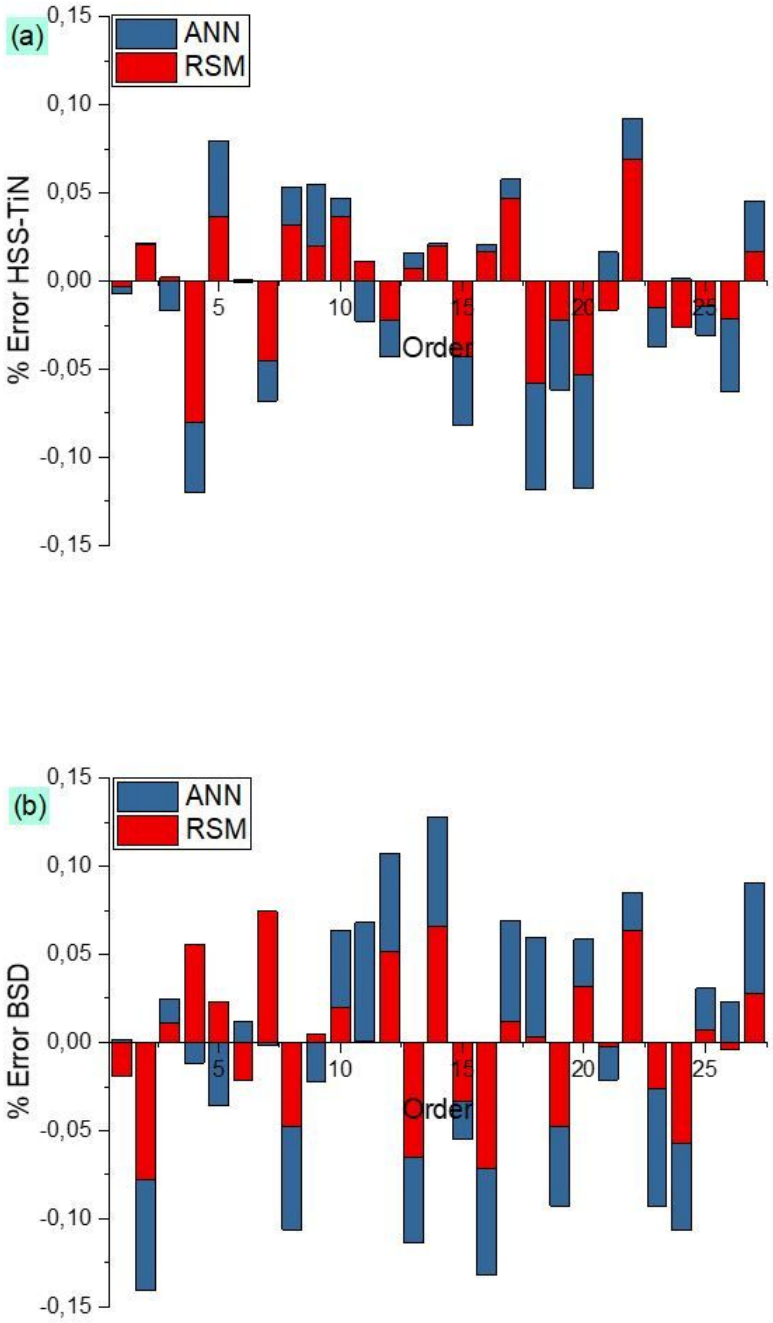

Figure 11

Fd residuals for RSM and ANN (a) HSS-TiN and (b) BSD drills.

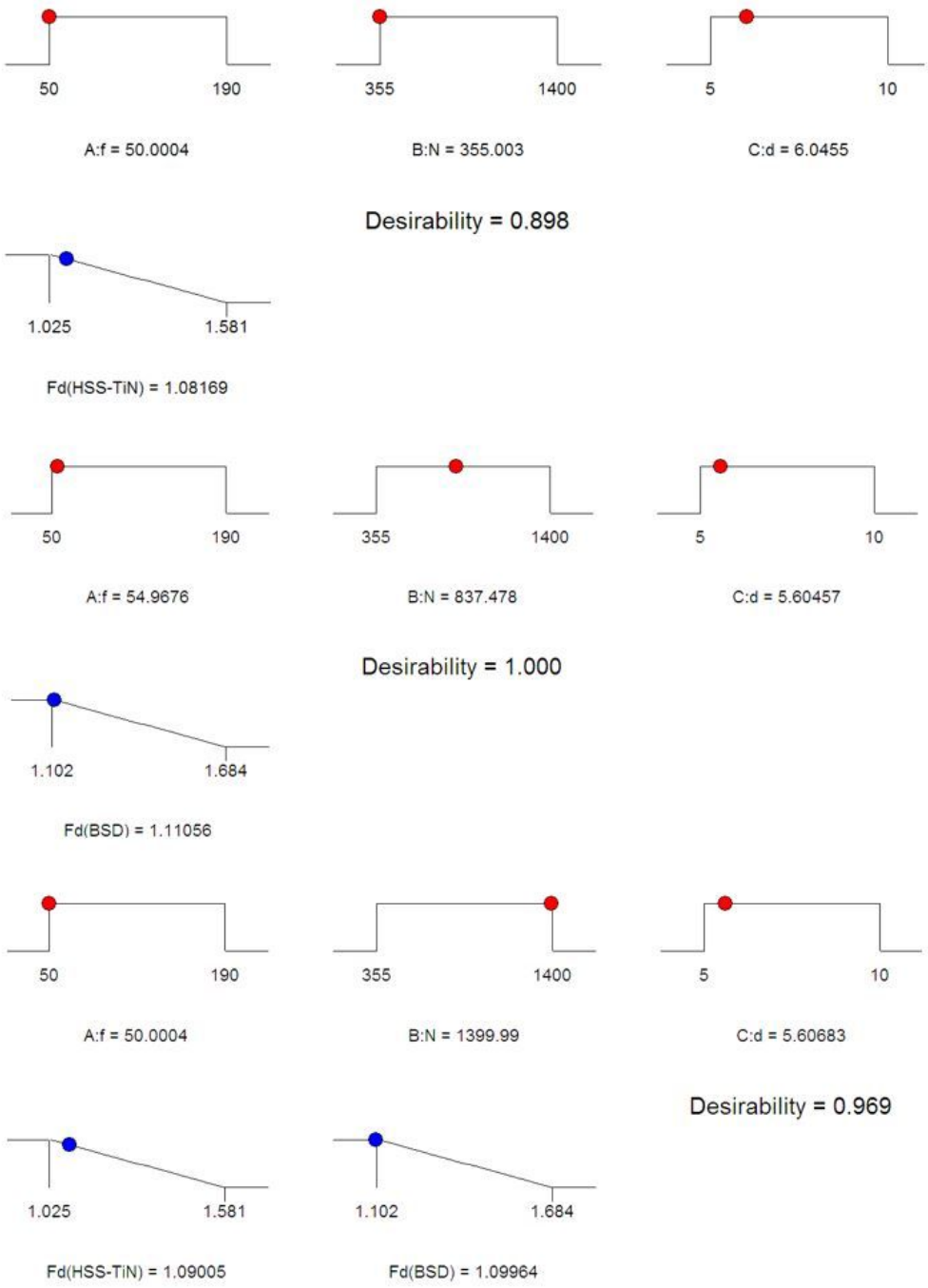

Figure 12

Ramp function graph of multi-objective optimization (a) HSS-TiN, (b) BSD and (c) HSS-TiN and BSD tools

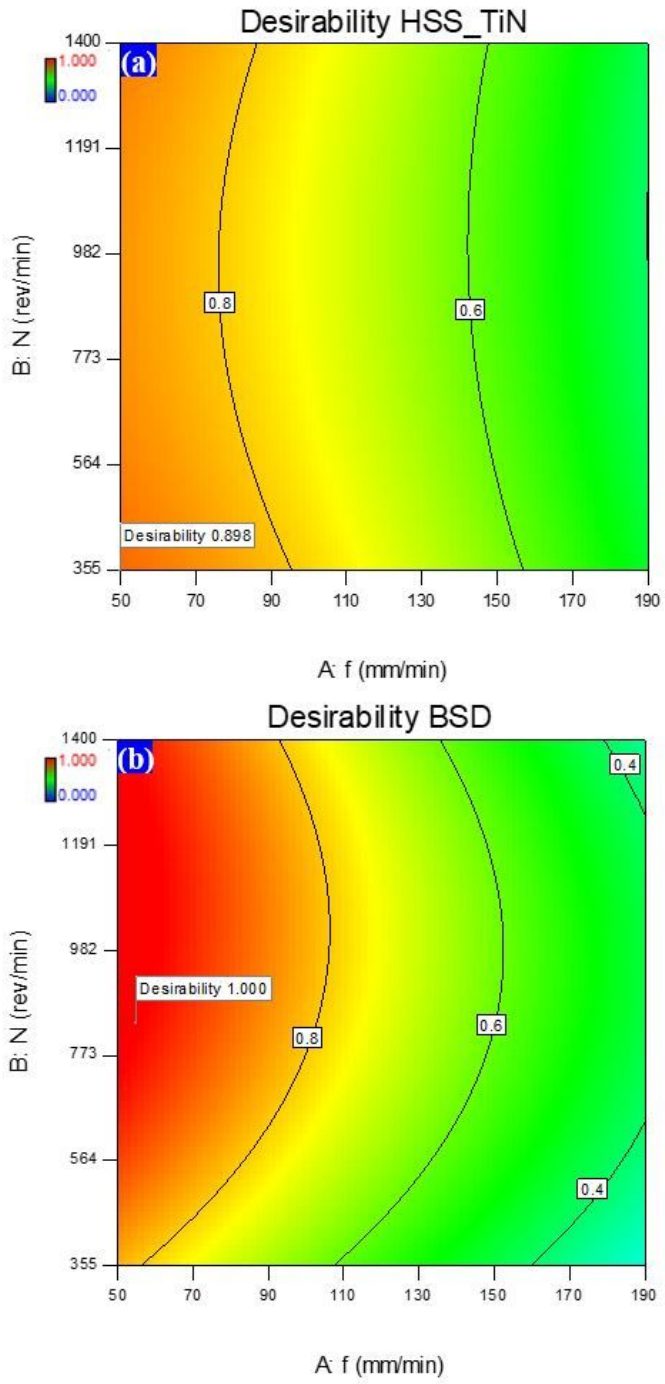

Figure 13

Contour plot of desirability for Fd for (a) HSS-TiN and (b) BSD tools.